Novel Skid Avoidance Method without Vehicle Chassis Speed for Electric Vehicle

Shin-ichiro Sakai , Hideo Sado and Yoichi Hori
University of Tokyo Department of Electrical Engineering
7-3-1 Hongo, Bunkyo, Tokyo 113-8656, Japan
Phone: +81-3-5841-7683, Fax: +81-3-5841-7683
E-Mail: sakai@hori.t.u-tokyo.ac.jp

Abstract

Novel wheel skid detection method without chassis velocity for electric vehicle (EV) is proposed. This method can sense the wheel skid with only the values of current and rotating velocity of motor. Estimation of vehicle chassis velocity is not required. The output torque of motor is easily comprehensible, and the proposed method utilizes this advantage of EV. The experiments were carried out and the results show the effectiveness of this method. We also discussed on the design of skid prevention controller with this skid detector. The designed controller was also examined with experimental results.

Key words: Electric Vehicle(EV), Vehicle Motion Control, Anti Skid Break System(ABS), Traction Control System(TCS)

1 Introduction

Electric Vehicle (EV) is evolving to be practical enough. Hybrid EV (HEV) like Toyota Prius is commercially succeeding, and Fuel cell EV (FCEV) will possibly be a major vehicle in the 21st century.

From the viewpoint of electric and control engineering, EV has three big advantages over ICV. First advantage is the fast and precise motor torque. This advantage of EV, the fast torque response, should enhance the performance of anti skid break system (ABS) or traction control system (TCS). Note that electric motor can accelerate and decelerate the wheel continuously, only depending on the sign of reference torque value. Thus in EV, ABS and TCS can be realized with only one actuator.

Second, the output torque of motor is easily comprehensible. This will be a great help for the estimation of vehicle motion, like chassis slip angle estimation [2] or maximum tire-road friction force monitoring [3] [4]. This paper also mainly studies on this advantage.

Third, individual torque of every driven wheel can be controlled independently, in such EV with in-wheel motors [5]. IZA [6] is equipped one in-wheel motor with every wheel, and Luciole [7] has one for each rear wheel. With independently controlled wheels, more effective chassis control like Direct Yaw Moment Control(DYC) [8][9] will be available.

With these advantage, the advanced motion control of electric vehicle should be studied, however, there are quite few researches [10] [11]. For example, these three advantages above will be utilized in an integrated control of each wheel and chassis. The typical purpose of such control is to enhance the vehicle stability, and the typical target situation is that the "2 wheel motored" or "4 wheel motored" EV turns the curve on slippery road with braking. One of the problems in such situation will be the measurement of slip ratio, since the vehicle chassis velocity cannot be estimated easily in such situation.

In this paper, novel skid detection method is proposed. This method can detect skid of driven wheel only with the values of motor current and rotating velocity. No information about wheel absolute velocity or vehicle chassis velocity is required. Therefore, this method is expected to improve the performance of anti skid control, which is cooperating with DYC. The controller with this novel skid detector is also discussed, and skid preventing experiments is carried out in the latter part of this paper.

2 Skid Detector without Wheel Absolute Velocity

In this section, novel method of skid detection is proposed. Slip phenomena of wheel is evaluated with the slip ratio λ, defined as

$$\lambda = \frac{r\omega - V}{r\omega} \tag{1}$$

for an accelerating wheel, where r, ω, V are the wheel radius, wheel rotating velocity and wheel absolute velocity [1]. Most ABS's or TCS's calculate this slip ratio to detect the skid of wheel. In order to calculate slip ratio, wheel absolute velocity or vehicle chassis speed is required. The vehicle chassis speed is sensed with measurement of chassis' acceleration or computed with the velocity of non-driven wheels approximately. This estimation is not so easy during the 4 wheel driving/braking, or when the vehicle turns the curve. Thus this paper proposes the skid detection method without chassis speed.

[1] Most usual variable for slip ratio is s, however λ is used here for slip ratio and s denotes Laplace operator.

To treat slip phenomena, simple one-wheel vehicle model (Fig. 1) is assumed. Motion equations of wheel and chassis in this model are

$$M_w \frac{dV_w}{dt} = F_m - F_d \quad (2)$$

$$M \frac{dV}{dt} = F_d \quad (3)$$

respectively, where

F_m	motor torque (force equivalent);
F_d	traction force;
M_w	wheel inertia (mass equivalent);
M	vehicle weight;
V_w	wheel rotating velocity (velocity equivalent);
V	vehicle velocity.

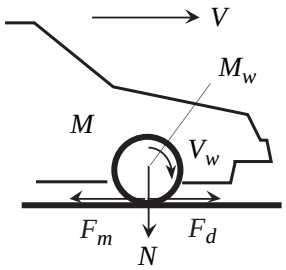

Figure 1. One wheel vehicle model.

F_d is the traction force, or friction force between the road and wheel. The normalized traction force μ is defined as the ratio of traction force F_d and normal force N on driven wheel,

$$\mu = \frac{F_d}{N}. \quad (4)$$

A plot of the normalized traction force μ versus the slip ratio λ shows a significant nonlinear characteristic which depends on the road conditions. Fig. 2 plots the examples of $\mu - \lambda$ curves for various road conditions, dry asphalt, wet asphalt and iced road.

The slip phenomena can be described with (1)-(4) and $\mu(\lambda)$ function. Then the following perturbation system is derived from these equations as,

$$\Delta\lambda = \frac{\partial\lambda}{\partial V}\Delta V + \frac{\partial\lambda}{\partial V_w}\Delta V_w = -\frac{1}{V_{w0}}\Delta V + \frac{V_0}{V_{w0}^2}\Delta V_w, \quad (5)$$

$$M_w \frac{d}{dt}\Delta V_w = \Delta F_m - \Delta F_d, \quad (6)$$

$$M \frac{d}{dt}\Delta V = \Delta F_d, \quad (7)$$

$$\Delta F_d = aN\Delta\lambda, \quad (8)$$

where $V_{\omega 0}$ and V_0 are the wheel and chassis velocity at the operational point. The $\mu - \lambda$ characteristic defined as

$$a \equiv \left.\frac{\partial\mu}{\partial\lambda}\right|_{\lambda_0}, \quad (9)$$

where λ_0 is the slip ratio at the operational point.

From (6)-(8), the transfer function from the motor torque F_m to the traction force F_d is finally given by

$$\frac{\Delta F_d}{\Delta F_m} = K\frac{1}{\tau_a s + 1}, \quad (10)$$

where the proportional gain K and time constant τ_a are given by

$$K = \frac{M(1-\lambda_0)}{M_w + M(1-\lambda_0)}, \quad (11)$$

$$\tau_a = \frac{M_w V_{w0}}{aN}\frac{M(1-\lambda_0)}{M_w + M(1-\lambda_0)}. \quad (12)$$

Here we set some $\mu - \lambda$ curve as an example, which has its maximum μ at $\lambda = 0.1$. Then calculate K and τ_a with this $\mu - \lambda$ curve, and plot them versus λ in Fig. 3. As (11), (12) and Fig. 3 show, these values depend on λ as

$K \simeq \frac{M}{M_w + M}$	for small λ (adhesive region),
$\tau_a \ll 1$	for small λ (adhesive region),
$\tau_a \gg 1$	when $\lambda \to 0.1$ (adhesive limit),
$\tau_a < 0$	when $\lambda > 0.1$ (skid region).

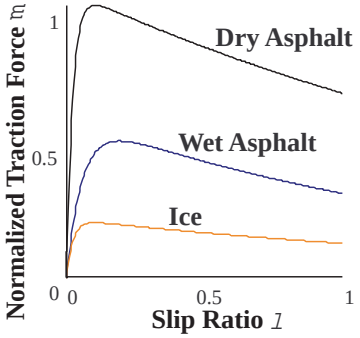

Figure 2. Examples of $\mu - \lambda$ curve.

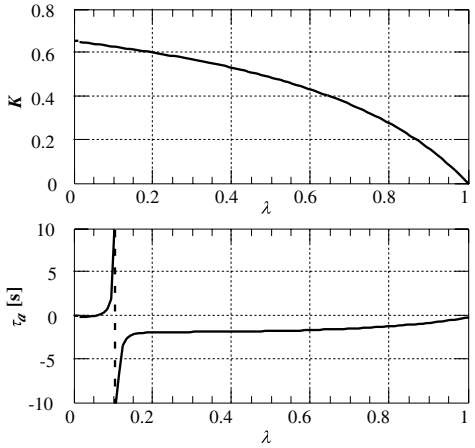

Figure 3. Examples of K and τ_a.

Consequently, we roughly describe these properties of slip phenomena as

$$\begin{cases} \dfrac{\Delta F_m}{\Delta F_d} = \dfrac{M}{M_w + M} & \text{(in adhesive region)}, \\ \dfrac{\Delta F_m}{\Delta F_d} \leq 0 & \text{(in skid region)}. \end{cases} \tag{13}$$

Based on these simple descriptions, we suppose that the gradient of $F_m - F_d$ curve g,

$$g \equiv \frac{dF_d}{dF_m}, \tag{14}$$

indicates the status of slip phenomena as

$$\begin{cases} g \simeq \dfrac{M}{M_w + M} & \text{(in adhesive region)}, \\ g \leq 0 & \text{(in skid region)}. \end{cases} \tag{15}$$

Note that g for adhesive wheel only depends on the vehicle weight and wheel inertia in this description.

To apply this method, the value of traction force F_d is required. In EV, usual disturbance observer(DOB) has enough performance to estimate F_d as a load torque[1] [12]. We call this estimator "traction force observer". Note again that it is quite easy to get the accurate value of motor torque.

2.3 Experiments of Skid Detector

Experiments of proposed skid detector were carried out with the laboratory-made experimental EV "UOT Electric March I". The specification of this vehicle is appeared in Table 1, and its configuration is depicted in Fig. 4. The motor torque is transmitted to the front wheels through clutch, reduction gears, and driving shaft. Since each rotating velocity of front and rear wheel is measured with shaft encoder, slip ratio λ can be calculated as a reference value.

Fig. 5 plots the time evolution of slip ratio λ for driven wheel, when the EV accelerated on the dry asphalt road. From this figure, the driven wheel is estimated to be skidding between 1-2[s]. Fig. 6 shows the $F_m - F_d$ curve obtained in this experiment. $\hat{F}_d$ is observed with traction force observer, which has a time constant of 100[ms]. Recursive least square (RLS) method was applied with forgetting factor to calculate the gradient g of this curve. Calculated g is plotted in Fig. 7. Dashed lines in Fig. 6 and Fig. 7 indicate the theoretical gradient for adhesive wheel calculated in (15). As Fig. 7 shows, the gradient g is about 0 or negative value when the wheel is skidding. In contrast, g is near or above the theoretical value for adhesive wheels, when the wheel is adhesive. These figures show the effectiveness of proposed skid detector, which sense the skid with g, the gradient of $F_m - F_d$ curve.

Max. Torque	85[Nm]
Gear Ratio	13.5
Battery	**Lead Acid**
Nominal Capacity	92[Ah]
Total Volt.	120[V] (with 10 units)
Chassis	**Nissan March**
Weight	1000[kg]
Wheel Inertia	21.1[kgm^2]*
Wheel Radius	0.26[m]
CPU	i386, 20[MHz]
Encoder(front/rear wheel)	1800 / 120[ppr]

* ... Including the rotor of motor, affected by gear ratio.

Table 1. Specifications of "UOT Electric March I".

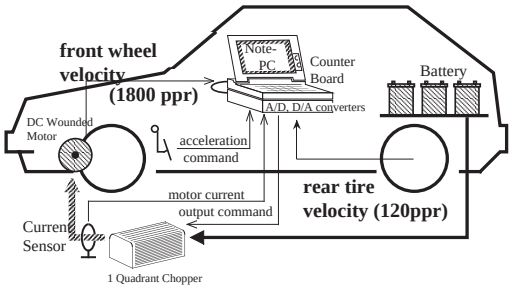

Figure 4. Configuration of UOT Electric March I

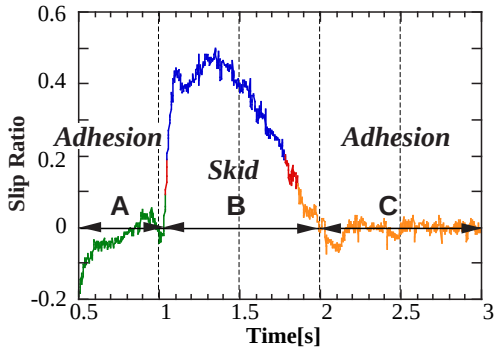

Figure 5. Slip ratio (experiment on dry asphalt).

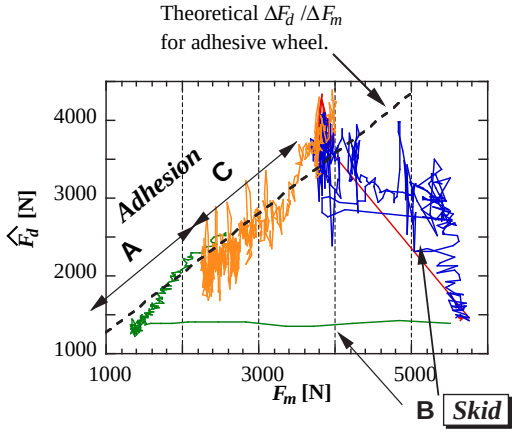

Figure 6. F_m-F_d curve (experiment on dry asphalt).

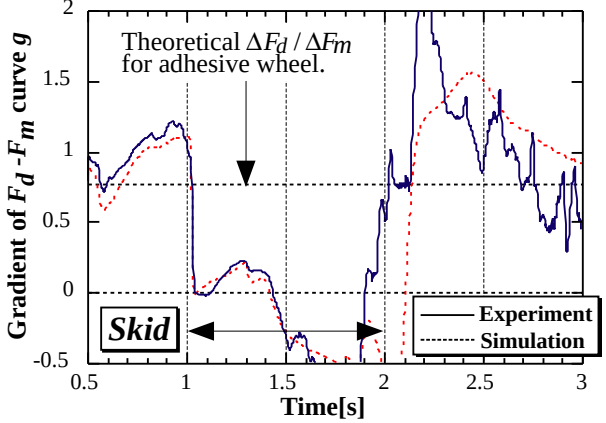

Figure 7. g, the gradient of F_m-F_d curve(experiment on dry asphalt).

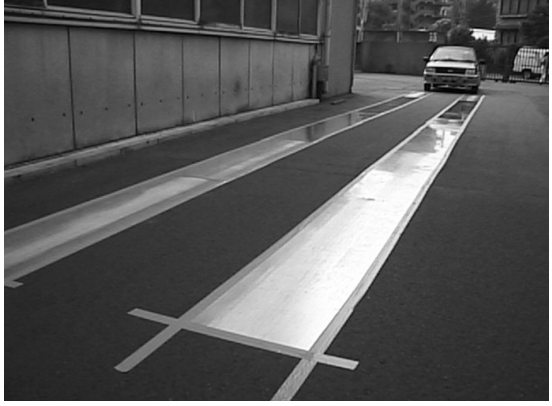

Figure 8. Low μ test road and "UOT Electric March I".

3 Anti Skid Control with Skid Detector

3.1 Design of Anti Skid Controller

In this section, anti skid controller is proposed based on the skid detector. The output of the skid detector is g, defined with (14) in the previous section. Following the (13), we change the control status in sequence as

$$\begin{cases} g > 0.0 & : \text{adhesive status,} \\ g \leq 0.0 & : \text{skid status,} \\ g \geq 0.5\gamma_M & : \text{re-adhesive status,} \end{cases} \tag{16}$$

where

$$\gamma_M = \frac{M}{M_w + M}. \tag{17}$$

The motor torque is equal to the human driver's input when skid detector output "adhesive" status, i.e., $g > 0.0$. Once $g < 0.0$, the controller decreases the motor torque exponentially until the status comes to be "re-adhesive", or g grows up over $0.5\gamma_M$. When the status is recovered to "re-adhesive", then the motor torque is again increased exponentially. For EV with DC motor such as UOT Electric March I, this algorithm can be rewritten with motor current I, as

$$\begin{cases} \dfrac{dI}{dt} = -\dfrac{I}{\tau} & : \text{in skid status,} \\ \dfrac{dI}{dt} = \dfrac{I_0 - I}{\tau} & : \text{in re-adhesive status.} \end{cases} \tag{18}$$

When the skid detector first senses the wheel skid, I_0 is initialized to be the motor current at that moment. In this paper, time constant τ is set to 150 [ms]. If the motor current is increased/decreased more rapidly, the skid detector cannot sense the skid or re-adhesion properly. This limit seems to depend on the time constant(100 [ms]) of traction force observer. When the skid detector's output changes from "skid" to "re-adhesive", the controller stops increasing the motor torque and decreases it in a instant. To eliminate the affect of this discontinuous derivative of motor torque, we stop the skid detection for 300[ms], when the status changes from "skid" to "re-adhesive".

3.2 Experiments of Anti Skid Control

Then this proposed anti skid controller was examined experimentally with UOT Electric March I. This slip experiment was carried out out on slippery road with wet aluminum plates of 14[m] long. Fig.8 is a photo of this experimental low μ road. In this experiment, motor current lineally increases with a slop of 240[A/s] until the wheel starts skidding. This current pattern substitute the human driver's input.

Fig. 9 shows the slip experimental results with this controller. Motor current I or motor torque lineally increases at first as shown in Fig. 9(a). This causes the slip ratio λ to increase as (c). When the λ becomes larger than about 0.2, the wheel skidding is sensed by the skid detector as (d), and the controller decreases motor current I until the skid detector senses re-adhesion. In result, the slip ratio λ oscillates around about 0.1, as shown in Fig. 9(c), and serious skid can be prevented.

Vehicle reached the end of this 14[m] low μ road at 5.2[s]. After 5.2[s] vehicle ran on the high μ dry asphalt, with decreasing slip ratio. Accordingly, after 5.2[s] skid detector continuously output "adhesive", thus the controller does not decrease the motor current. Fig. 9 (a) indicates that the actual motor current dropped at 5.1[s]. This was caused by the voltage saturation of battery, with large back electro motive force of DC motor at high speed region.

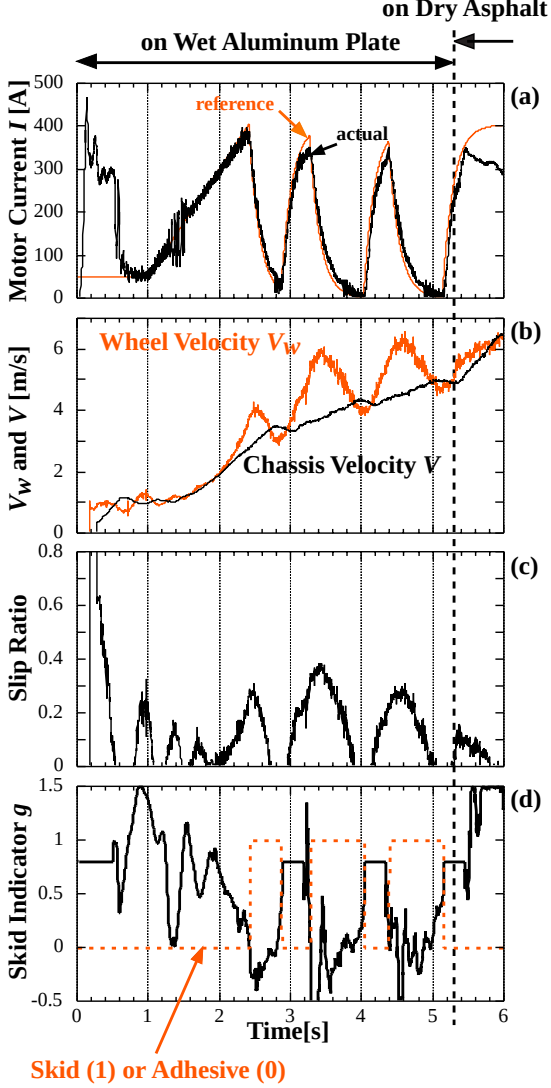

Figure 9. Experimental results of anti skid control.

3.3 Evaluation of Proposed Anti Skid Controller

For evaluation of proposed anti skid controller, we tried to observe the $\mu-\lambda$ curve of the test low μ road, controlling the slip ratio with slip ratio control [1]. The driving force F_d were calculated with MdV/dt in these experiments, and plotted vs. slip ratio in Fig. 10. This experimentally observed $\mu-\lambda$ curve has some error bar, however, we can still estimate that this road has maximum driving force 1800∼2000 [N] at $\lambda \simeq 0.1$. Therefore, it was confirmed that the proposed anti skid controller could almost maintain the slip ratio around its optimal value.

In results, the effects of proposed controller can be mentioned as,

1. serious skid and unstable vehicle lateral motion could be prevented,
2. and the driving or breaking force was enlarged.

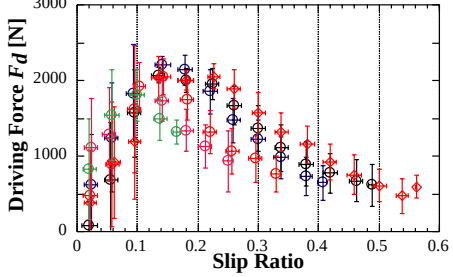

Figure 10. Experimentally Observed road $\mu-\lambda$ curve.

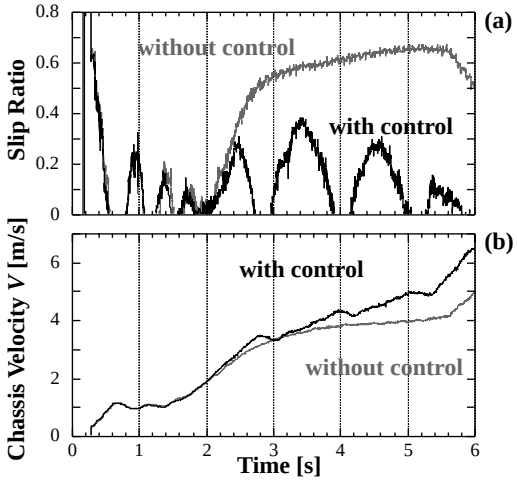

Figure 11. Effect of proposed anti skid control.

Fig. 11 shows these effects clearly. These figures are the comparison of experimental results with and without proposed anti skid controller. Without controller, serious skid of $\lambda \simeq 0.6$ occurred as shown in Fig. 11 (a). This serious situation could be avoided with proposed method, enlarging the the driving force F_d. Fig. 11 (b) shows this effect with comparison of vehicle chassis velocity.

On the contrary, proposed method could not maximize the driving force. From Fig. 10, the maximum driving force can be estimated to be about 1800 [N] for this experimental low μ road. The average chassis acceleration from 2[s] to 5.3[s] in Fig. 9 was 0.98[m/s^2]. The mass of body is about 1100[kg], therefore, average driving force in this experiments was about 1100[N]. Thus the achieved driving force with anti skid controller is about 60% of its maximum value.

In this paper, we carried out only acceleration experiments, since UOT Electric March I has only one quadrant chopper, or has no regenerating brake. In the usual EV, the regeneration brake is generally applied. Then the proposed method will also be available for skid prevention during electric braking. In such case, minimization of braking distance is an importance issue. The driving force maximization in accelerating vehicle has the same meaning of the braking force maximization in decelerating vehicle.

maximization is desirable. To maximize the driving force, optimal slip ratio should be continuously achieved. The problem is slow estimation of the skid detector. It requires more than 100 [ms], relatively larger than motor's torque response of 2 $\sim$ 3 [ms]. We are now discussing about fast minor feedback control of motor velocity, such as model following control (MFC) [1].

4 Conclusions

In this paper, novel skid detection method for electric vehicle (EV) was proposed and discussed. This proposed method can detect skid of wheel with only the values of current and rotating velocity of each motor. In other words, only the information of motor itself is required. Estimation of vehicle chassis velocity or wheel absolute velocity is not required any more, and this is remarkable advantage over conventional methods.

In this proposed method, traction force is estimated with simple "traction force observer", thus the exact value of shaft input torque is required. It is quite easy in EV. As we pointed out, this is one of the advantages of EV for vehicle motion control.

The proposed algorithm was examined experimentally with laboratory-made electric vehicle "UOT Electric March I". These experimental results show the effectiveness of proposed skid detection method. The design of anti skid controller based on this skid detector was also studied in this paper. Another experimental results show the effectiveness of this controller.

Proposed skid detector requires no information about vehicle chassis velocity or slip ratio, thus this method should be significantly effective for skid avoidance during the cornering motion. This anti skid controller will be integrated and examined with our new experimental EV "UOT Electric March II" (Fig. 12) [13], which has independently controlled four in-wheel motors. Cooperative control of proposed skid prevention method and DYC, control of vehicle chassis motion with torque difference, still remains for further studies. It will be studied experimentally with our new EV.

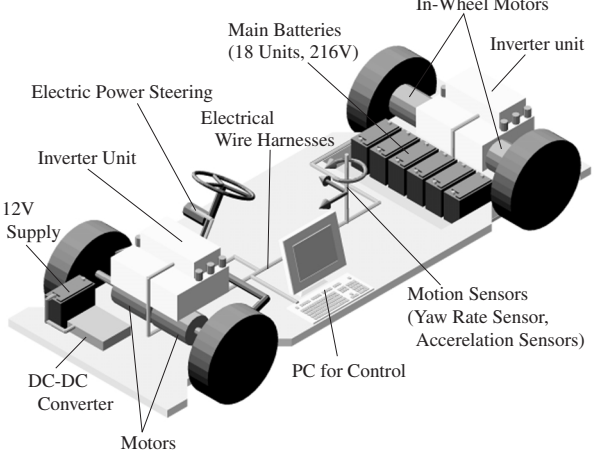

Figure 12. Configuration of our new EV.

References

[1] Y. Hori, Y. Toyoda, and Y. Tsuruoka, "Traction control of electric vehicle: Basic experimental results using the test EV "UOT electric march"," *IEEE Trans. Ind. Applicat.*, vol. 34, no. 5, pp. 1131–1138, 1998.

[2] U. Kiencke and A. Daiss, "Observation of lateral vehicle dynamics," *Control Eng. Practice*, vol. 5, no. 8, pp. 1145–1150, 1997.

[3] F. Gustafsson, "Monitoring tire-road friction using the wheel slip," *IEEE Control Systems Magazines*, vol. 18, no. 4, pp. 42–49, 1998.

[4] F. Gustafsson, "Slip-based tire-road friction estimation," *Automatica*, vol. 33, no. 6, pp. 1087–1099, 1997.

[5] T. Ashikaga, M. Mori, T. Mizuno, K. Nagayama, T. Kobayashi, and T. Kubo, "High efficiency induction motor control method for electric vehicle," in *Proc. IPEC'95*, Yokohama, 1991, pp. 113–118.

[6] H. Shimizu et al., "The concept and simulation of a high performance EV IZA," in *Proc. EVS. 11 no.5,*, 1992.

[7] H. Shimizu, J. Harada, C. Bland, K. Kawakami, and C. Lam, "Advanced concepts in electric vehicle design," *IEEE Trans. Ind. Electron.*, vol. 44, no. 1, pp. 14–18, 1997.

[8] Yasuji Shibahata et al., "The improvement of vehicle maneuverability by direct yaw moment control," in *Proc. AVEC '92*, 1992, number 923081.

[9] M. Abe et al., "Estimation of vehicle side-slip angle for DYC by using on-board tire model," in *Proc. 4th International Symposium on Advanced Vehicle Control*, Nagoya, 1998, pp. 437–442.

[10] P.Khatun, C.M.Bingham, P.H.Mellor, and N.Schofield, "Discrete-time ABS/TC test facility for electric vehicles," in *Proc. EVS. 16*, Beijing, 1999, p. 75.

[11] Y. Wang and M. Nagai, "Integrated control of four-wheel-steer and yaw moment to improve dynamic stability margin," in *Proc. 35th IEEE Conf. Decision and Control*, Kobe, 1996, pp. 1783–1784.

[12] K. Ohishi, K. Nakano, I. Miyashita, and S. Yasukawa, "Anti-slip control of electric motor coach based on disturbance observer," in *Proc. 5th Advance Motion Control*, Coimbra, 1998, pp. 580–585.

[13] S. Sakai, "Project of motion control in an electric vehicle with four in-wheel motors," URL: http://www.hori.t.u-tokyo.ac.jp/997/sakai/Research/index.html, 1999.